Electron Paramagnetic Resonance Study of the $[W(CO)_4\{P(OMe)_3\}]^-$ Radical Anion trapped in a Single Crystal of $[N(PPh_3)_2][W(CO)_4H\{P(OMe)_3\}]$†

Rosemary C. Hynes, Keith F. Preston,* Jerry J. Springs, and Antony J. Williams
Steacie Institute for Molecular Sciences, National Research Council of Canada, Ottawa, Ontario K1A 0R9, Canada

Gamma-irradiated single crystals of $[N(PPh_3)_2][W(CO)_4H\{P(OMe)_3\}]$ contain an anisotropic e.p.r. signal which exhibits hyperfine coupling to a single ^{31}P nucleus. *X*-Ray crystallography showed that the crystals belonged to the orthorhombic system (*Pbca*), with a = 15.562 6(21), b = 19.980(3), c = 27.161(4) Å, and Z = 8; the undamaged anion had an approximately octahedral geometry in which the H atom was *cis* to the phosphite ligand. Crystallographically aligned specimens were used to determine both the $\boldsymbol{g}$ and the ^{31}P hyperfine interaction tensors [$\boldsymbol{g}$ = 2.0708, 2.0740, 1.9914; $\boldsymbol{a}(^{31}P)$ = 75.1, 68.4, 45.5 MHz] and their direction cosines in the crystal-axis system. The form of the $\boldsymbol{g}$ tensor and the alignment of $g_{min.}$ with the H–W–C$_{ax.}$ direction of the undamaged anion point to considerable unpaired spin density in the W $5d_{z^2}$ orbital. Alignment of the ^{31}P tensor along $g_{min.}$ and the W–P bond is attributed to direct overlap of the P $3p_z$ orbital with the metal atomic orbital. Comparison with other ^{31}P hyperfine measurements suggests that e.p.r. provides a good indication of the efficiency of back-bonding in such organometallic radicals.

The past decade has seen a rapid growth in the generation and spectroscopic characterization of open-shell organotransition-metal compounds, to the point where stable (persistent) species of that type now constitute an important subdivision of transition-metal chemistry.[1] From a structural point of view, open-shell five-co-ordinate mononuclear complexes are a particularly interesting group because of the variety of nearly equienergetic conformations which they offer.[2] Moreover, they are frequently important intermediates along the reaction pathway between four- and six-co-ordinate complexes. Our interest in this area stems from our detection[3,4] by e.p.r. spectroscopy of paramagnetic impurity centres in $Cr(CO)_6$ crystals, which we ascribed to the cation and anion radicals of $Fe(CO)_5$.

Spectroscopic studies of metal pentacarbonyl free radicals were frustrated at the outset by the failure to detect an e.p.r. spectrum of the prototypical d^7 species, $Mn(CO)_5$, in the liquid phase.[5–10] Its spectrum has since been detected in the solid state,[11–13] as have those of certain isoelectronic radical cations[3,14] and anions of neighbouring group metals,[15,16] but the liquid-phase spectrum remains elusive. The solid-state spectroscopic data show[3,11–16] beyond any reasonable doubt that the d^7 transition-metal carbonyls of Groups 6—8 have a square-pyramidal geometry with unpaired electron spin density largely confined to the metal valence d_{z^2} orbital, as predicted in the seminal papers of Burdett[17,18] and Hoffmann and co-workers.[19,20] Unfortunately, lack of sign information[3,13] for the experimental ^{13}C hyperfine tensors prevented an unequivocal determination of the ligand-orbital contributions to the semioccupied molecular orbital (s.o.m.o.). Considerations[13] of the ^{13}C couplings for $Mn(CO)_5$ in a krypton matrix suggested that, as predicted theoretically,[20] unpaired spin density in ligand orbitals was confined to the equatorial carbonyl ligands rather than uniquely to the axial carbonyl, the alternative favoured in an earlier[3] experimental study of $Fe(CO)_5{}^+$. The measurement of ^{31}P hyperfine couplings tensors for phosphine-substituted metal carbonyl radicals would appear to offer a solution to this problem. Phosphorus-31 ($I = \frac{1}{2}$, 100% abundance) has large one-electron magnetic parameters[21] which make it a particularly useful probe of unpaired spin density, and the requisite transition-metal carbonyl phosphines[22] are well established starting materials. An added incentive to such an investigation is the possibility of detecting a change in geometry upon substituting carbonyls by phosphines. There is already strong spectroscopic evidence[23,24] that the disubstituted iron carbonyl cation has a trigonal-bipyramidal geometry. This paper describes the crystal structure of $[N(PPh_3)_2][W(CO)_4H\{P(OMe)_3\}]$, and a single-crystal e.p.r. spectroscopic study of the monosubstituted tungsten carbonyl radical anion produced by ionizing radiation; we also review the electronic structure of square-pyramidal organotransition-metal pentacarbonyl radicals in light of the findings.

Experimental

(*a*) *Preparation.*—The complex $[N(PPh_3)_2][W(CO)_4H\{P(OMe)_3\}]$ was prepared according to published procedures.[25] Single crystals of the material were obtained by layering a concentrated tetrahydrofuran solution of the hydride with hexane and cooling it to −20 °C. Solvents were purified by distillation from sodium diphenylketyl, or purchased as reagent grade; they were degassed immediately prior to use and stored over molecular sieves.

(*b*) *Crystallography.*—An Enraf-Nonius CAD diffractometer controlled by NRCCAD software[26] was used for the collection of *X*-ray diffraction data (Table 1). The structure was solved by direct methods. With the exception of the hydride ion, hydrogen atoms were included in the structure-factor calculations in idealized positions based on C–H 1.08 Å, the bond length suggested by past experience with the refinement of hydrocarbon structures. The hydride was located in a difference map and its positional parameters were refined. The structure was refined by cycles of least-squares calculations using weights based on counting statistics. Data reduction, structure solution and refinement were all carried out using the NRCVAX system

---

† Bis(triphenylphosphine)iminium tetracarbonyl(hydrido)(trimethyl phosphite)tungstate(0).

Supplementary data available: see Instructions for Authors, *J. Chem. Soc., Dalton Trans.*, 1990, Issue 1, pp. xix—xxii.

Non-S.I. units employed: eV ≈ 1.60 × 10^{-19}J, G = 10^{-4}T.

Table 1. Summary of *X*-ray diffraction data

Compound	$[N(PPh_3)_2][W(CO)_4H\{P(OMe)_3\}]$
Formula	$C_{43}H_{40}NO_7P_3W$
M	959.55
Crystal system	Orthorhombic
Space group	*Pbca*
a/Å	15.562 6(21)[a]
b/Å	19.980(3)[a]
c/Å	27.161(4)[a]
U/Å^3	8 445.2(21)
Z	8
D_c/g cm^{-3}	1.509
Crystal dimensions/mm	0.20 × 0.20 × 0.10
T/°C	24
λ(Mo-K_α)/Å	0.709 30
μ(Mo-K_α)/mm^{-1}	2.95
Data collection	ω—2θ
$2\theta_{max.}$/°	44.7
Scan speed/° min^{-1}	2
Scan width/°	1
Total no. observations	8 062
No. unique observations	5 444
No. unique data, $I > 2.5\sigma(I)$	3 048
Final no. variables	344
Final max. shift/error	0.189
Max. residual density/e Å^{-3}	1.41 (0.05 Å from W)
Secondary extinction coefficient	0.467(14)
Goodness of fit	2.49
R^b for data where $I > 2.5\sigma(I)$	0.052
R'^c for data where $I > 2.5\sigma(I)$	0.028
R^b for all data	0.114
R'^c for all data	0.031

[a] Calculated from 25 reflections with 2θ in the range 30—35°. [b] $\Sigma||F_o| - |F_c||/\Sigma|F_o|$. [c] $[\Sigma w(|F_o| - |F_c|)^2/\Sigma wF_o^2]^{\frac{1}{2}}$.

of crystal structure programs.[27] Atomic co-ordinates for the non-hydrogen atoms appear in Table 2, and selected bond distances, angles, and directions are given in Table 3.

Additional material available from the Cambridge Crystallographic Data Centre comprises H-atom co-ordinates, thermal parameters, and remaining bond lengths and angles.

Single crystals were irradiated at 77 K in a 400 TBq ^{60}Co source for 4 h. Since the radicals generated were stable at room temperature for several days, it was possible to prealign crystals for e.p.r. spectroscopy absolutely on a Picker diffractometer according to the structural parameters. These crystals were glued inside the ends of 4-mm quartz tubes such that one of the orthogonal axes *abc* of the *Pbca* orthorhombic crystal lay parallel to the length of the tube. The direction of a second crystal axis was indicated by a pointer attached at right angles to the tube. Contact of the crystals with air was minimized by coating them with epoxy glue in a dry-box prior to alignment.

(*c*) *E.P.R. Spectroscopy*.—E.p.r. spectra were recorded with a Varian Associates E-12 spectrometer equipped with standard accessories for the measurement of magnetic field intensity and microwave frequency.[28] Each prealigned irradiated crystal in turn was held *via* its quartz supporting tube at the centre of the microwave cavity of the spectrometer in a cold-finger Dewar filled with liquid nitrogen. A horizontal brass protractor graduated every 5° of arc lay immediately underneath the pointer attached to the quartz tube. By rotation of the tube about its long axis the magnetic field of the spectrometer could then explore a crystallographic plane. Three separate planes, *ab*, *ac*, and *bc*, were explored together with a skew direction in order to establish the matrices of magnetic parameters in the basis of the orthorhombic unit cell.[29]

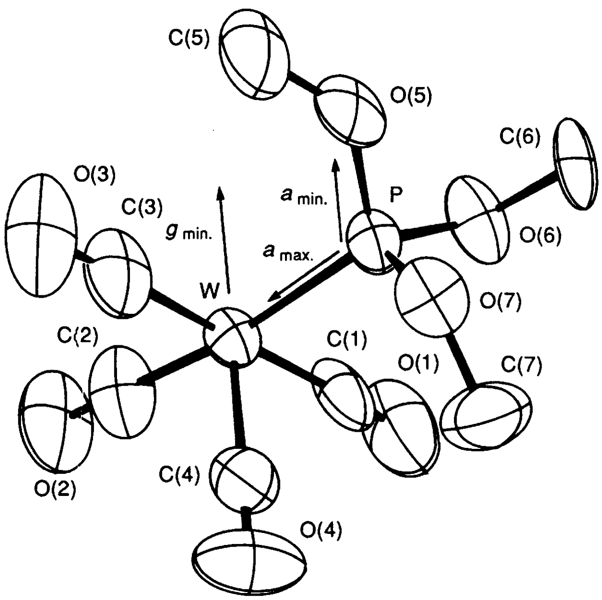

Figure 1. Structure of the $[W(CO)_4H\{P(OMe)_3\}]^-$ anion (omitting the hydrogen atom) as determined by *X*-ray crystallography, showing the principal directions of certain components of the g and ^{31}P hyperfine interaction tensors

Results

The *X*-ray diffraction study of $[N(PPh_3)_2][W(CO)_4H\{P(OMe)_3\}]$ showed that the crystal was orthorhombic (*Pbca*) with $Z = 8$. The structure of the $[N(PPh_3)_2]^+$ cation was unremarkable;[30] the anion had nearly perfect octahedral geometry about a central tungsten atom and a *cis* arrangement of the hydride and phosphite ligands (Figure 1). This structure corroborated the inferences from earlier infrared and ^{13}C n.m.r. studies.[25]

For an arbitrary orientation of the d.c. magnetic field the e.p.r. spectrum of a γ-irradiated single crystal of $[N(PPh_3)_2][W(CO)_4H\{P(OMe)_3\}]$ consisted of eight lines of equal intensity. This spectrum coalesced to a pair of lines when a crystal axis was aligned along B_0, and to four lines when B_0 lay in a crystal plane (Figure 2). The simplest spectrum observed thus consisted of a doublet which was attributed to a ^{31}P hyperfine coupling. The angular dependence of the spectrum is typical of 'site splitting' in an orthorhombic crystal[29] in which each of four magnetically inequivalent sites gives rise to a hyperfine doublet.

The g factors and the ^{31}P hyperfine coupling (a_{31}) were measured to first order throughout the three crystal planes and for the 'skew' direction ($1/\sqrt{3}$, $1/\sqrt{3}$, $1/\sqrt{3}$).[29] The scalar measures of the tensors $\boldsymbol{g}^2$ and $\boldsymbol{g}\cdot\boldsymbol{a}\cdot\boldsymbol{a}\cdot\boldsymbol{g}$, g^2, and g^2a^2, were calculated for each direction and were plotted as a function of angular displacement from a crystal axis for each plane (Figures 3 and 4). The expected sinusoidal behaviour was observed within each crystal plane. Matrix elements of the $\boldsymbol{g}^2$ tensors were obtained from[29] least-squares fits of expressions of the type $g^2(\theta) = g_{xx}{}^2\cos^2\theta + g_{yy}{}^2\sin^2\theta + g_{xy}{}^2\sin2\theta$ to the experimental data. From the four values of g measured for the ($1/\sqrt{3}$, $1/\sqrt{3}$, $1/\sqrt{3}$) direction (2.0719, 2.0631, 2.0404, 2.0070), it was established that the off-diagonal signs in $\boldsymbol{g}^2$ were all negative (or any one negative).[29] Diagonalisation of $\boldsymbol{g}^2$ led to the principal values and directions in the crystal *abc* basis which are summarized in Table 4. In the case of the $\boldsymbol{g}\cdot\boldsymbol{a}\cdot\boldsymbol{a}\cdot\boldsymbol{g}$ tensor, the off-diagonal signs were established by comparison of the plots for g^2 and g^2a^2; the tensor was then pre- and post-multiplied by $\boldsymbol{g}^{-1}$ in the crystal basis to yield $\boldsymbol{a}^2$. Principal values and directions for the hyperfine interaction are also given in Table 4.

Table 2. Atomic co-ordinates for $[N(PPh_3)_2][W(CO)_4H\{P(OMe)_3\}]$ with estimated standard deviations in parentheses

Atom	*x*	*y*	*z*
W	0.519 70(4)	0.194 44(3)	0.062 708(18)
P(1)	0.495 1(3)	0.281 57(16)	0.002 00(13)
P(2)	0.980 6(3)	0.022 19(14)	0.167 73(10)
P(3)	0.913 51(24)	−0.046 02(16)	0.256 56(12)
O(1)	0.411 9(8)	0.273 9(5)	0.138 7(4)
O(2)	0.575 5(7)	0.103 6(5)	0.149 9(3)
O(3)	0.645 0(8)	0.112 8(6)	−0.002 2(4)
O(4)	0.367 8(7)	0.105 1(6)	0.030 8(4)
O(5)	0.571 0(7)	0.306 2(5)	−0.033 6(3)
O(6)	0.423 8(7)	0.273 8(4)	−0.040 7(3)
O(7)	0.468 3(7)	0.351 3(4)	0.026 33(24)
N	0.976 6(6)	−0.026 3(4)	0.213 2(3)
C(1)	0.450 8(10)	0.245 6(7)	0.108 2(5)
C(2)	0.553 2(10)	0.137 1(7)	0.116 4(4)
C(3)	0.595 0(12)	0.146 2(8)	0.022 0(5)
C(4)	0.425 0(10)	0.138 7(8)	0.043 2(6)
C(5)	0.643 1(11)	0.274 2(8)	−0.049 4(6)
C(6)	0.333 5(10)	0.259 8(8)	−0.028 7(5)
C(7)	0.449 5(9)	0.410 4(6)	−0.001 6(4)
C(11)	0.976 9(10)	−0.067 2(5)	0.308 6(4)
C(12)	0.939 6(9)	−0.082 5(6)	0.353 7(5)
C(13)	0.993 0(10)	−0.098 8(6)	0.392 4(4)
C(14)	1.0797(10)	−0.100 9(6)	0.388 2(5)
C(15)	1.116 2(9)	−0.086 9(6)	0.344 3(5)
C(16)	1.065 4(9)	−0.070 4(6)	0.304 3(4)
C(21)	0.840 6(7)	0.018 2(5)	0.275 5(4)
C(22)	0.860 9(8)	0.059 4(6)	0.315 5(4)
C(23)	0.805 7(9)	0.113 5(6)	0.325 3(4)
C(24)	0.736 7(9)	0.126 3(6)	0.295 4(4)
C(25)	0.717 5(9)	0.087 7(6)	0.255 2(5)
C(26)	0.770 9(9)	0.032 8(5)	0.245 6(5)
C(31)	0.848 6(8)	−0.116 7(5)	0.239 7(4)
C(32)	0.777 8(9)	−0.134 2(6)	0.267 7(4)
C(33)	0.729 5(9)	−0.190 9(6)	0.254 3(5)
C(34)	0.752 6(9)	−0.227 9(6)	0.213 6(4)
C(35)	0.822 2(8)	−0.210 3(6)	0.184 7(4)
C(36)	0.871 1(8)	−0.155 5(6)	0.199 2(4)
C(41)	0.983 2(8)	0.108 8(5)	0.185 5(3)
C(42)	1.001 4(8)	0.126 1(5)	0.233 6(3)
C(43)	1.006 6(8)	0.192 5(6)	0.248 4(4)
C(44)	0.994 1(9)	0.241 7(5)	0.213 9(4)
C(45)	0.975 7(9)	0.227 2(6)	0.166 5(4)
C(46)	0.969 5(9)	0.159 7(5)	0.150 8(4)
C(51)	0.894 3(8)	0.011 1(6)	0.124 3(4)
C(52)	0.823 3(8)	0.053 1(6)	0.123 1(4)
C(53)	0.756 7(9)	0.040 1(7)	0.090 2(4)
C(54)	0.762 1(8)	−0.013 0(6)	0.061 0(5)
C(55)	0.830 2(8)	−0.057 8(5)	0.061 6(5)
C(56)	0.897 9(8)	−0.045 5(6)	0.094 0(4)
C(61)	1.077 6(7)	0.003 6(6)	0.135 8(4)
C(62)	1.111 4(8)	−0.059 3(6)	0.138 8(4)
C(63)	1.183 8(8)	−0.076 3(6)	0.111 0(4)
C(64)	1.225 1(8)	−0.029 3(6)	0.083 0(4)
C(65)	1.190 2(8)	0.032 6(6)	0.080 0(4)
C(66)	1.116 3(8)	0.051 6(6)	0.105 6(4)
H(W)	0.610(4)	0.224(3)	0.064 4(25)

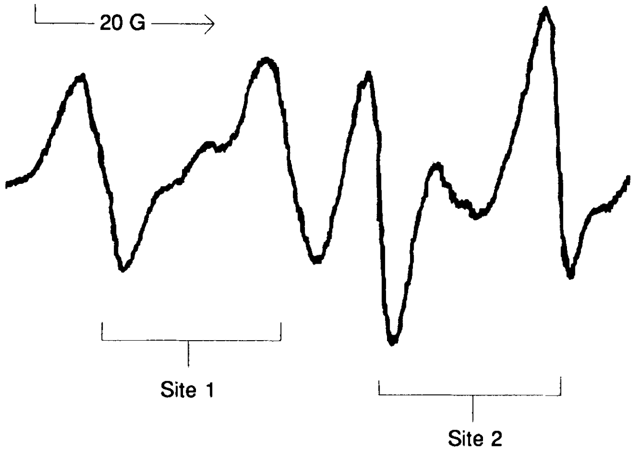

Figure 2. First-derivative e.p.r. spectrum of a γ-irradiated single crystal of $[N(PPh_3)_2][W(CO)_4H\{P(OMe)_3\}]$ at 77 K (9056.5 MHz) for an orientation where B_0 lies 20° from *a* in the *ac* plane

Discussion

The space group *Pbca* generates eight symmetry-equivalent sites which are related in pairs by an inversion centre. Since e.p.r. is blind to inversion,[29] the observation of a 'four-site' spectrum for an arbitrary direction in the crystal shows that the impurity centre obeys the crystal space group. It is reasonable, therefore, to assume that the paramagnetic centre is substitutional, and to look for correlations of tensor principal directions with crystallographic directions in the undamaged ions. A close correspondence was in fact (Table 5) found between principal directions of *g* and a_{31} and certain directions within the undamaged anions. There can be little doubt, therefore, that the paramagnetic impurity derives from the host anion, and the following considerations show that it is the square-pyramidal radical resulting from hydrogen atom loss.

Table 3. Selected bond distances (Å) and angles (°) for $[N(PPh_3)_2]$-$[W(CO)_4H\{P(OMe)_3\}]$

W–C(1)	1.929(14)	W–C(2)	1.927(13)
W–C(3)	1.877(16)	W–C(4)	1.922(16)
W–H	1.53(6)	W–P(1)	2.428(3)
O(1)–C(1)	1.171(17)	O(2)–C(2)	1.182(15)
O(3)–C(3)	1.219(19)	O(4)–C(4)	1.164(19)
C(1)–W–C(2)	88.9(6)	C(1)–W–C(3)	175.0(7)
C(1)–W–C(4)	93.3(7)	C(1)–W–H	106.7(24)
C(2)–W–C(3)	88.4(6)	C(2)–W–C(4)	94.1(6)
C(2)–W–H	87.6(24)	C(3)–W–C(4)	91.1(8)
C(3)–W–H	69.0(25)	C(4)–W–H	160.0(25)

Directions

	a	*b*	*c*
W–P(1)	0.1577	−0.7169	0.6791
W–C(1)	0.5558	−0.5299	−0.6405
W–C(4)	0.7669	0.5795	0.2757

The absence of fine structure from the spectrum and the proximity of the principal *g* values to that of a free spin (2.0023) show that the spectrum has its origin with a single unpaired electron ($S = \frac{1}{2}$). Interaction of the unpaired electron with a single ^{31}P nucleus ($I = \frac{1}{2}$, 100% natural abundance) gives rise to the doublet structure of the spectrum. The principal values of the *g* tensor (Table 4) are very similar to those[15,16] of $W(CO)_5^-$ trapped in $[N(PPh_3)_2][W(CO)_5H]$ or 2-methyltetrahydrofuran. Furthermore, just as in that radical, $g_{min.}$ is aligned very nearly along the H–W–$C_{ax.}$ direction of the undamaged anion. The *g* tensor is almost cylindrical, more nearly so, in fact, than that of the parent $W(CO)_5^-$ radical[16] in $[N(PPh_3)_2][W(CO)_5H]$ ($g_{xx} = 2.0791$, $g_{yy} = 2.0671$, $g_{zz} = 1.9925$). For this reason, the principal directions of *g* in the perpendicular plane of the radical are ill defined and do not correlate well with bond directions in the undamaged anion.

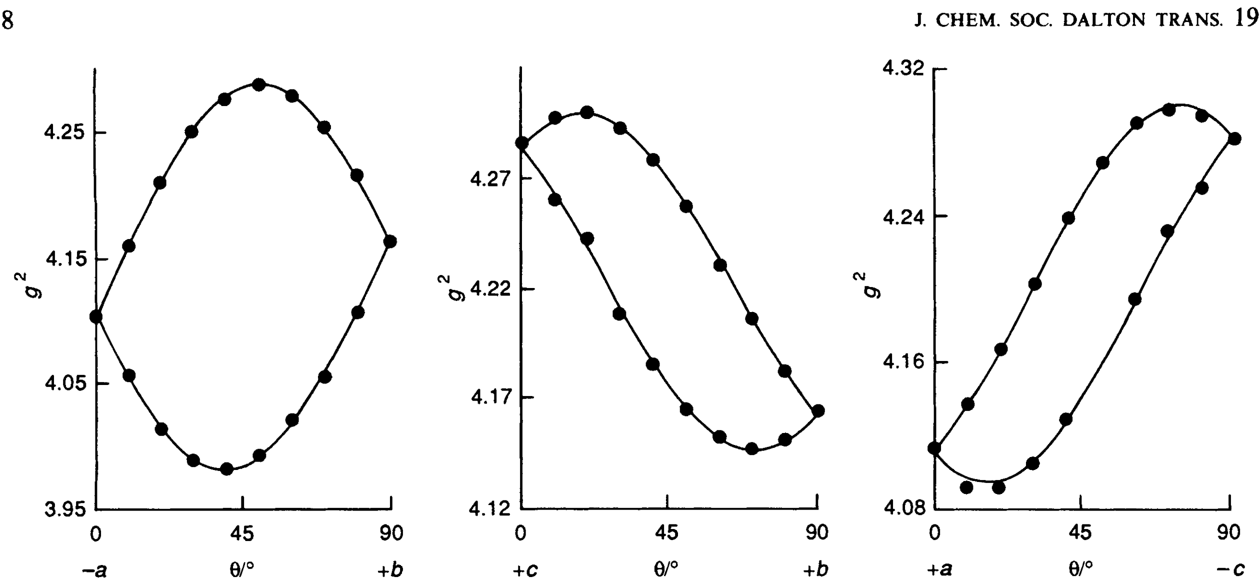

Figure 3. Plots of g^2 against angle for the three crystal planes, and least-squares best-fit curves to the data

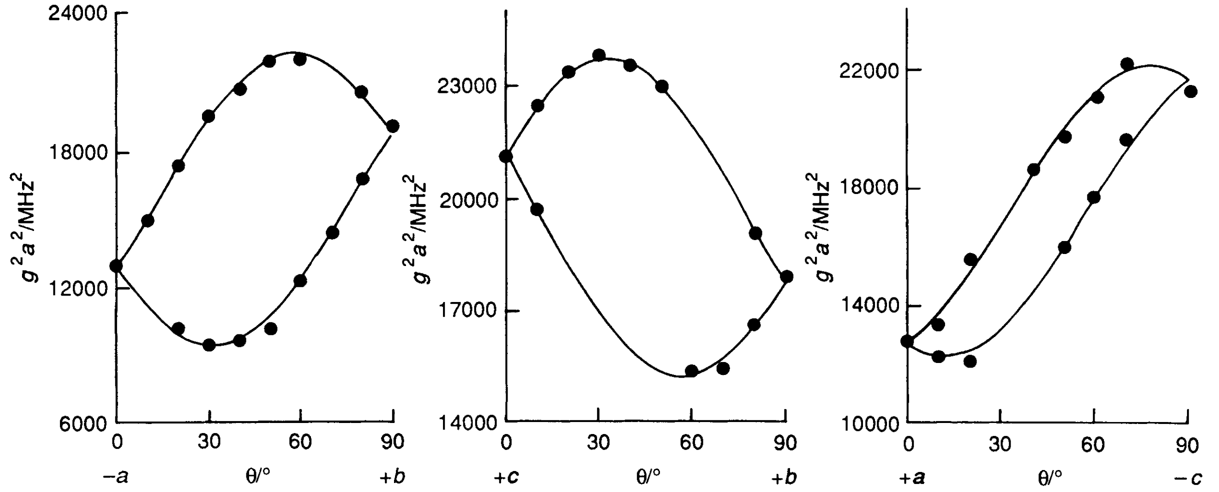

Figure 4. Plots of g^2a^2 against angle for the three crystal planes, and least-squares best-fit curves to the data

Table 4. The g^2 and $g{\cdot}a^2{\cdot}g$ (MHz^2) tensors for the $[W(CO)_4\{P(OMe)_3\}]^-$ radical in a single crystal of $[N(PPh_3)_2][W(CO)_4H\{P(OMe)_3\}]$; principal values of g and ^{31}P hyperfine interaction (MHz) and their direction cosines in the *abc* axis system

	Tensor*			$g_x = 2.0708$	$g_y = 2.0740$	$g_z = 1.9914$
	a	*b*	*c*	0.6392	−0.1819	0.7472
	4.1085	−0.1506	−0.0563	−0.7689	−0.1316	0.6257
g^2	−0.1506	4.1621	−0.0469	0.0155	0.9745	0.2240
	−0.0563	−0.0469	4.2845			
					$a(^{31}P)$	
				75.1	68.4	45.5
	12 950	−5 637	−2 071	0.1881	0.5879	0.7867
$g{\cdot}a^2{\cdot}g$	−5 637	18 193	−3 815	−0.6578	−0.5194	0.5454
	−2 071	−3 815	21 357	0.7293	−0.6202	0.2891

* Off-diagonal signs appropriate for one of the four sign combinations which correspond to the four magnetically inequivalent sites observed experimentally.

The shifts of the g values from the free-spin value ($g_{\parallel} < g_e$, and $g_{\perp} \gg g_e$) and the near-axiality of the tensor clearly point to a s.o.m.o. with an important contribution from the W $5d_{z^2}$ orbital. The positive shifts for g in the equatorial plane (Figure 1) arise through spin-orbit coupling of the half-filled metal d_{z^2} level with a pair of filled levels (Figure 5) that have their origin with the degenerate *e* ($d_{xz,yz}$) pair of levels in C_{4v} geometry. Judging by the near-axiality of g, the substitution of a phosphite ligand for an equatorial carbonyl (Figure 1), with consequent lowering of the symmetry to C_s, would appear to have caused very little splitting of the $d_{xz,yz}$ pair. This is at first sight a most surprising inference, since the *xz*,*yz* pair are generally believed[31] to be strongly overlapped with ligand π orbitals, and we would expect significant differences in bonding efficiency between a CO and a $P(OMe)_3$ ligand. However, using the spin-orbit coupling parameter of tungsten[32] and the expression,[33] $\Delta g_\perp = 6\zeta/\Delta E$, where E = energy and ζ = spin–orbit coupling constant, we estimate energy gaps of 1 and 22.7 eV between *xz* and *yz* and between z^2 and *xz*, respectively. Even though these estimates are upper limits calculated for unit unpaired spin density in both ground and excited orbitals, they illustrate the point that deviations from axiality of *g* in this situation are insensitive to bonding changes in the perpendicular plane. For similar reasons, the small differences in *g* values between the phosphite-substituted radical and the parent radical (see above) do not imply a negligible electronic effect of the substituent on the s.o.m.o. A more sensitive measure of any such effect is given by changes in the metal hyperfine interaction which, unfortunately, could not be measured for either species.

Isotropic or average ^{31}P hyperfine couplings in phosphine- or phosphite-substituted organotransition-metal radicals fall typically[1] in the range 10—30 G, values which translate[21] into less than 1% P 3*s* character. Estimation of P 3*p* character in such radicals requires careful consideration of the anisotropic ^{31}P tensors which unfortunately are only available in a few instances. In Table 6 we give the isotropic and anisotropic components of ^{31}P tensors derived from hyperfine determinations for a number of 17-electron metal-centred radicals having phosphine or phosphite ligands.[34—38] For the purposes of discussion, we have initially assumed that the tensor components are either all positive or all negative, according to the rationale given below. Contributions to the ^{31}P hyperfine coupling in such radicals arise from three sources: (*i*) positive unpaired spin density through direct P 3*s* or 3*p* character of the s.o.m.o., (*ii*) negative spin density in those orbitals through polarization of the metal–phosphorus bond by the metal *d* orbital,[39] (*iii*) a through-space, purely dipolar interaction due to the unpaired spin at the metal nucleus.[40] We choose to ignore inner *s* terms due to core polarization because of the small spin densities in the P 3*p* orbital. Furthermore, from the *g* anisotropies of these radicals, we estimate that contributions to the ^{31}P hyperfine interaction from the orbital magnetic moment are quite negligible.[41]

For a metal–phosphorus bond of 2.4 Å, *i.e.* the W–P distance in the title anion, the dipolar ^{31}P hyperfine contribution is of the form (4, −2, −2 MHz), with the maximum value along the bond. We have divided the radicals of Table 6 into two sets according to the size of the anisotropic component of the ^{31}P tensor: those which have an anisotropic component commensurate with a purely dipolar interaction, and those with much larger anisotropy. The first entry in Table 6, *trans*-$[V(CO)_4(PMe_3)_2]$, is distinct from the others in that direct *s* character on the phosphorus nuclei is symmetry forbidden.[34] The dominant isotropic contribution to the ^{31}P hyperfine interaction is, therefore, expected to be a *negative* bond polarization term. Since the anisotropic component of largest absolute magnitude (5.0 MHz) in this instance lies along the metal–phosphorus bond, it is tempting to reverse all of the signs to give a positive

Table 5. Correlation between tensor principal directions and directions within the undamaged metal carbonyl anion

Tensor component	Angle to W–C$_4$ (°)	Angle to W–C$_1$ (°)	Angle to W–P (°)
$g_{\text{min.}}$	4.2	93.4	100.3
$a_{\text{min.}}$ ^{31}P	2.4	92.1	94.0
$a_{\text{inter.}}$	91.2	2.3	87.5
$a_{\text{max.}}$	92.0	90.8	4.8

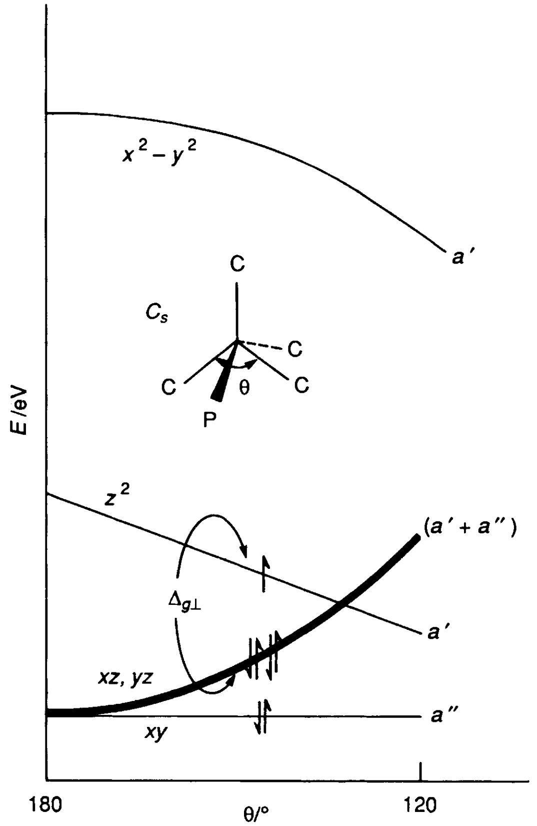

Figure 5. *d*-Block orbitals for $[W(CO)_4\{P(OMe)_3\}]^-$ in C_s symmetry, adapted from the scheme for C_{4v} symmetry of ref. 19

Table 6. ^{1}P Hyperfine interaction tensors for certain organotransition-metal radicals

Radical	^{31}P hyperfine tensor (MHz) $a_{\text{iso.}}$	a_{xx}	a_{yy}	a_{zz}	Reference
trans-$[V(CO)_4(PMe_3)_2]$	−86.1	4.8	0.2	−5.0	34
$[Mn(\eta\text{-}C_4H_6)_2(PMe_3)]$	−74.4	3.4	0.0	−3.4	35
$[Mn(CO)_3(PPr^i{}_3)_2]$	−58.0	0.0	0.0	0.0	37
$[Mn(CO)_3\{P(OPr^i)_3\}_2]$	−73.0	−5.0	−5.0	10.0	37
$[W(CO)_4\{P(OMe)_3\}]^-$	−63.0	−12.1	−5.4	17.5	This work
fac-$[V(CO)_3(PMe_3)_3]$	76.0	−17.0	−17.0	34.0	36
$[Co(tpp)(PMe_3)]$*	667.0	−33.0	−33.0	66.0	38

* tpp = 5,10,15,20-Tetraphenylporphyrinate.

expected for purely dipolar interaction. However, the former argument based on symmetry considerations is compelling to our minds, and we feel strongly that the sign choice for *trans*-[$V(CO)_4(PMe_3)_2$] is correct. An exactly analogous situation arises in phosphobetaine radical cations and related species,[42,43] where an unpaired electron in a C 2*p* orbital is believed to give rise to negative spin density in the α P 3*s* orbital and sufficient negative spin density in the α P 3*p* orbital directed along the bond to swamp the dipolar term. By contrast, in the remaining entries for the first group of radicals, direct P 3*s* character is permitted, yet both the isotropic and anisotropic components remain small. The similarity in size of their isotropic hyperfine couplings to that in *trans*-[$V(CO)_4(PMe_3)_2$] convinces us that they also are negative, due to spin polarization of the metal–phosphorus bond, and that direct *s* contributions are negligible. In [$Mn(\eta\text{-}C_4H_6)_2(PMe_3)$], the phosphine is apical in a square-pyramidal arrangement about the Mn nucleus; the unpaired electron is located in the Mn $3d_{z^2}$ orbital. It would appear, somewhat surprisingly, yet totally in accord with theoretical predictions,[20] that the apical ligand is barely implicated, if at all, in the a_1 s.o.m.o. Even more surprising is the lack of participation of phosphorus orbitals from the *basal* ligands in [$Mn(CO)_3(PPr^i_3)_2$], where overlap between the Mn $4p_z$ and the P $3p_z$ orbitals is anticipated.[20] The rationale for these observations[37,42] presumably lies in a nearly perfect sp^3 hybridization of the P orbitals in the phosphine ligands: these ligands are poor π acceptors, and back-bonding into P 3*p* orbitals is negligible.

Turning now to the second group of radicals (Table 6), we note that the last entry for the 5,10,15,20-tetraphenylporphyrinatocobalt(II) complex has a ^{31}P tensor typical of a classical 'σ' radical, with significant positive spin density in the axial phosphorus 3*s* and 3*p* orbitals. The complex *fac*-[$V(CO)_3(PMe_3)_3$] has somewhat smaller couplings, but the size of the anisotropic components still clearly points to positive spin density (≈5%) in each of the P 3*p* orbitals. Both of these radicals have totally symmetric ground-state wavefunctions[36,38] to which admixture of P 3*s* and 3*p* is permitted. The complex [$Mn(CO)_3\{P(OPr^i)_3\}_2$] and [$W(CO)_4\{P(OMe)_3\}$]$^-$, the radical under investigation, have very similar ^{31}P hyperfine interaction tensors. This is not too surprising since both radicals are square–pyramidal with the phosphorus ligands in basal positions and the unpaired electron essentially localised in the metal d_{z^2} orbital. Our choice of all ^{31}P tensor elements as being negative for these cases (Table 6) is consistent with the choice made for the similar species [$Mn(CO)_3(PPr^i_3)_2$] and [$Mn(\eta\text{-}C_4H_6)_2(PMe_3)$], and leads to the prediction of positive unpaired spin density (≈2%) in the P $3p_z$ orbital. Overlap between the metal p_z orbital and basal ligand p_z atomic orbitals is expected,[20] as mentioned above, although it is weak in the case of the phosphine ligands. Increased back-bonding is expected as the groups attached to phosphorus become more electronegative and the ligand becomes a better π acceptor.[31]

Conclusion

Gamma-irradiation of [$N(PPh_3)_2$][$W(CO)_4H\{P(OMe)_3\}$] results in hydrogen-atom loss from the anion and the formation of a tungsten-centred free radical which retains the geometry of the undamaged $W(CO)_4\{P(OMe)_3\}$ moiety, *i.e.* square pyramidal with the phosphite ligand in the equatorial plane. The substitution of a phosphite ligand in the equatorial plane of the parent radical $W(CO)_5^-$ has little influence on the *g* tensor components, but these are judged to be insensitive indicators of bonding changes in this example. The ^{31}P hyperfine coupling to the unpaired electron is anisotropic and sufficiently large to suggest direct overlap of the W $5d_{z^2}$ orbital with the P $3p_z$, as anticipated from the theoretical s.o.m.o. for the parent radical. The absence of this type of bonding in the case of phosphine substitution is inferred from earlier measurements which indicate an almost isotropic ^{31}P hyperfine interaction. Such hyperfine determinations thus provide a direct measure of the extent of back-bonding and support the indirect, but long established,[31] inferences drawn from carbonyl infrared stretching frequencies.

Acknowledgements

The authors are indebted to Mr. R. Dutrisac of these laboratories for his technical assistance.

References

1 M. C. Baird, *Chem. Rev.*, 1988, **88**, 1217.
2 T. A. Albright, J. K. Burdett, and M-H. Whangbo, 'Orbital Interactions in Chemistry,' Wiley, New York, 1985, ch. 17.
3 T. Lionel, J. R. Morton, and K. F. Preston, *J. Chem. Phys.*, 1982, **76**, 234.
4 S. A. Fairhurst, J. R. Morton, and K. F. Preston, *J. Chem. Phys.*, 1982, **77**, 5872.
5 E. O. Fischer, E. Offhaus, J. Muller, and D. Nothe, *Chem. Ber.*, 1972, **105**, 3027.
6 S. A. Hallock and A. Wojcicki, *J. Organomet. Chem.*, 1973, **54**, C27.
7 C. L. Kwan and J. K. Kochi, *J. Organomet. Chem.*, 1975, **101**, C9.
8 S. A. Fieldhouse, B. W. Fullam, G. W. Neilson, and M. C. R. Symons, *J. Chem. Soc., Dalton Trans.*, 1974, 567.
9 A. Hudson, M. F. Lappert, and B. K. Nicholson, *J. Organomet. Chem.*, 1975, **92**, C11.
10 A. S. Huffadine, B. M. Peake, B. H. Robinson, J. Simpson, and P. A. Dawson, *J. Organomet. Chem.*, 1976, **121**, 391.
11 J. A. Howard, J. R. Morton, and K. F. Preston, *Chem. Phys. Lett.*, 1981, **83**, 226.
12 M. C. R. Symons and R. L. Sweany, *Organometallics*, 1982, **1**, 834.
13 S. A. Fairhurst, J. R. Morton, R. N. Perutz, and K. F. Preston, *Organometallics*, 1984, **3**, 1389.
14 T. Lionel, J. R. Morton, and K. F. Preston, *J. Magn. Reson.*, 1982, **49**, 225.
15 P. J. Krusic, *J. Am. Chem. Soc.*, in the press.
16 R. Hynes, J. R. Morton, K. F. Preston, J. J. Springs, and A. J. Williams, *Organometallics*, 1990, **9**, 2298.
17 J. K. Burdett, *J. Chem. Soc., Faraday Trans. 2*, 1974, 1599.
18 J. K. Burdett, *Adv. Inorg. Chem. Radiochem.*, 1978, **21**, 113.
19 A. Rossi and R. Hoffmann, *Inorg. Chem.*, 1975, **14**, 365.
20 M. Elian and R. Hoffmann, *Inorg. Chem.*, 1975, **14**, 1058.
21 J. R. Morton and K. F. Preston, *J. Magn. Reson.*, 1978, **30**, 577.
22 H. J. Plastas, J. M. Stewart, and S. O. Grim, *J. Am. Chem. Soc.*, 1969, **91**, 4326; C. A. Tolman, *Chem. Rev.*, 1977, **77**, 313.
23 P. K. Baker, N. G. Connelly, B. M. R. Jones, J. P. Maher, and K. R. Somers, *J. Chem. Soc., Dalton Trans.*, 1980, 579.
24 M. J. Therien and W. C. Trogler, *J. Am. Chem. Soc.*, 1986, **108**, 3697.
25 S. G. Slater, R. Lusk, B. F. Schumann, and M. Y. Darensbourg, *Organometallics*, 1982, **1**, 1662.
26 Y. Le Page, P. S. White, and E. J. Gabe, American Crystallographic Association Annual Meeting, Hamilton, Ontario, 1986, Abstracts, p. 24.
27 E. J. Gabe, F. L. Lee, and Y. Le Page, 'Crystallographic Computing 3,' Clarendon, Oxford, 1985, p. 167.
28 J. R. Morton, K. F. Preston, and M. Y. Darensbourg, *Magn. Res. Chem.*, 1988, **26**, 787.
29 J. R. Morton and K. F. Preston, *J. Magn. Reson.*, 1983, **52**, 457.
30 L. B. Handy, J. K. Ruff, and L. F. Dahl, *J. Am. Chem. Soc.*, 1970, **92**, 7327.
31 F. A. Cotton and G. Wilkinson, 'Advanced Inorganic Chemistry,' 5th edn., Wiley, New York, 1988, ch. 2.
32 B. A. Goodman and J. B. Raynor, *Adv. Inorg. Chem. Radiochem.*, 1970, **13**, 192.
33 N. M. Atherton, 'Electron Spin Resonance,' Wiley, New York, 1973, p. 197.
34 J. M. McCall, J. R. Morton, and K. F. Preston, *Organometallics*, 1985, **4**, 1272.
35 J. M. McCall, J. R. Morton, and K. F. Preston, *Organometallics*, 1984, **3**, 1299.

36 J. M. McCall, J. R. Morton, and K. F. Preston, *J. Magn. Reson.*, 1985, **64**, 414.

37 G. B. Rattinger, R. L. Belford, H. Walker, and T. L. Brown, *Inorg. Chem.*, 1989, **28**, 1059.

38 B. B. Wayland and M. E. Abd-Elmageed, *J. Am. Chem. Soc.*, 1974, **96**, 4809.

39 H. M. McConnell and D. B. Chestnut, *J. Chem. Phys.*, 1958, **28**, 107.

40 H. M. McConnell and J. Strathdee, *Mol. Phys.*, 1959, **2**, 129.

41 N. M. Atherton and A. J. Horsewill, *J. Chem. Soc., Faraday Trans. 2*, 1980, **76**, 660.

42 A. Begum, A. R. Lyons, and M. C. R. Symons, *J. Chem. Soc. A*, 1971, 2388.

43 E. A. C. Lucken and C. Mazeline, *J. Chem. Soc. A*, 1967, 439; *ibid.*, p. 1074; M. Geoffroy, L. Ginet, and E. A. C. Lucken, *Mol. Phys.*, 1974, **28**, 1289; T. Berclaz and M. Geoffroy, *ibid.*, 1976, **32**, 815.

Received 7th March 1990; *Paper* 0/01025A